VI International Conference on Computational Methods for Coupled Problems in Science and Engineering
COUPLED PROBLEMS 2015
B. Schrefler, E. Oñate and M. Papadrakakis(Eds)

NUMERICAL SIMULATION OF GEOCHEMICAL COMPACTION WITH DISCONTINUOUS REACTIONS

Abramo Agosti*, Luca Formaggia*, Bianca Giovanardi* and Anna Scotti*

*MOX, Dipartimento di Matematica "F. Brioschi"
Politecnico di Milano
Via Bonardi 9, 20133 Milano, Italy
e-mail: mox@mate.polimi.it, web page: http://mox.polimi.it/

Key words: Compaction processes, discontinuous RHS ODE, mineral dissolution/precipitation.

Abstract. The present work deals with the numerical simulation of porous media subject to the coupled effects of mechanical compaction and reactive flows that can significantly alter the porosity due to dissolution, precipitation or transformation of the solid matrix. These chemical processes can be effectively modelled as ODEs with discontinuous right hand side, where the discontinuity depends on time and on the solution itself. Filippov theory can be applied to prove existence and to determine the solution behaviour at the discontinuities. From the numerical point of view, tailored numerical schemes are needed to guarantee positivity, mass conservation and accuracy. In particular, we rely on an event-driven approach such that, if the trajectory crosses a discontinuity, the transition point is localized exactly and integration is restarted accordingly.

1 Introduction

We propose a model to describe and simulate the compaction process under a progressive burial of a layer of sediments in which a mineral can dissolve in the water flow and precipitate on the grains of the rock. On one hand, compaction is due to the burial of the layer, which makes the overburden increase. On the other, the presence of the precipitated mineral can affect the solid matrix porosity, since the dissolving mineral may leave some void spaces, whereas the precipitated mineral may fill them. Moreover, an alteration of porosity implies a variation of permeability that affects the pressure of the water flowing through the rock layer. Again, fluid pressure counteracts compaction reducing the effective vertical stress, which has an effect on porosity. Finally, the chemical reactions that cause minerals to dissolve and precipitate are influenced by the fluid flow, which transports the solute.

The result is a nonlinear system of strongly coupled equations. The flow is assumed to obey Darcy's law. We use a simplified description of chemical reactions to model the

precipitation and dissolution of a mineral, such as quartz, see [7, 11, 2]. The effect of the fluid-solid conversion on porosity is accounted for by modifying Athy's constitutive law for the porosity [1], following [15, 16]. Again, we follow the strategy proposed in [15] and recast the governing equations in a Lagrangian frame. We simulate the sedimentation process by providing a sedimentation rate that causes the overburden to increase.

The system is solved by splitting the stronger coupling between pressure and compaction from the solution of the advection-diffusion-reaction equation for the transported solute. One main issue is that the equation that models the reaction of the mineral is a differential equation with discontinuous right hand side [10]. This led us to introduce another splitting between the advection-diffusion part of this equation and the reaction one, to take advantage of the available *ad hoc* methods to manage the discontinuity. In particular, among the possible strategies such as time step adaptation [8], or regularization of the right hand side [4], we chose to adopt an event-driven approach where the crossing of the discontinuity is exactly localized before restarting integration [5].

The paper is structured as follows. In Section 2 we present the mathematical model and we recast it into a Lagrangian frame. Section 3 deals with the numerical approach. In particular, we dwell on the application of a method to treat ODEs with discontinuous right hand side to our specific case. Finally in Section 4 the numerical solution obtained in one test configuration is analyzed, while conclusions are drawn in Section 5.

2 The model

We consider a layer of a sedimentary rock subject to a progressive burial. We assume that the porous medium is saturated with water. We are interested in modeling the behavior of a reactive material that can be advected by the flow when dissolved in water, and precipitate on the grains surface in the rocks. On the other hand, the precipitated mineral may dissolve into the fluid. It is clear that this mechanism, together with the increasing load due to the burial of the layer, affects the porosity ϕ of the sediments, leading to both geochemical and mechanical compaction.

2.1 The domain

We consider a two-dimensional model of the aforementioned processes, simulated in a vertical cross section of a sedimentary layer. Due to compaction, the domain of interest Ω evolves during the simulation. However, it is more convenient to cast the coupled problem of fluid flow, compaction and chemical reactions in a fixed geometry. For this reason, under the assumption that compaction acts only vertically, we define a fixed domain $\hat{\Omega}$, obtained from $\Omega = \Omega(t)$, as its completely compacted configuration once removed the reactive (dissolvable) part of the rock.

More precisely, following [15] and [16], we assume that one can define at any point $\boldsymbol{x} \in \Omega(t)$ and at any time the field $C = C(\boldsymbol{x}, t)$, which represents the ratio between the volume of the reactive part of the rock and the initial rock volume, so that the map

$\boldsymbol{\varphi}_t : \hat{\Omega} \to \Omega(t)$, $(x, \xi) \mapsto (x, z(\xi, t))$, is well defined and depends on C and ϕ. The deformation gradient $\boldsymbol{F}$ associated to this map is

$$\boldsymbol{F} := \nabla \boldsymbol{\varphi}_t = \begin{bmatrix} 1 & 0 \\ \partial z/\partial x & \partial z/\partial \xi \end{bmatrix}, \tag{1}$$

and it can be shown that the Jacobian is

$$J := \det(\boldsymbol{F}) = \frac{\partial z}{\partial \xi} = \frac{1 - C_0 + C}{(1 - C_0)(1 - \phi)} > 0, \tag{2}$$

where $C_0(\boldsymbol{x}) = C(\boldsymbol{x}, 0)$.

Note that the time derivative of the map coincides with the velocity $\boldsymbol{u}_s$ of the sediments and that, due to the hypothesis of vertical compaction, one has $\boldsymbol{u}_s = u_{sz}\boldsymbol{e}_z$, being $\boldsymbol{e}_z$ the unit vector of the z-axis.

2.2 Governing equations

In this section we present the equations governing the porous matrix evolution, fluid flow and chemical reactions in the fixed domain $\hat{\Omega}$. See [9] for a detailed derivation of the model.

The generic scalar field f in Ω becomes $\hat{f} = f \circ \boldsymbol{\varphi}_t$ in $\hat{\Omega}$, and the generic vector field $\boldsymbol{v}$ is transformed through the Piola transformation, that is $\hat{\boldsymbol{v}} = \hat{J}\, \hat{\boldsymbol{F}}^{-1} \boldsymbol{v} \circ \boldsymbol{\varphi}_t$, where $\hat{J}$ and $\hat{\boldsymbol{F}}$ are the transformation of (1) and (2) in $\hat{\Omega}$. Finally, the nabla operator in the fixed coordinate system is indicated with $\hat{\nabla}$.

If we assume that no water is released or consumed during the reactions, mass conservation for the fluid phase reads

$$\frac{\partial(\hat{\phi}\hat{\rho}_w \hat{J})}{\partial t} + \hat{\nabla} \cdot (\hat{\phi}\hat{\rho}_w \hat{\boldsymbol{u}}) = 0 \qquad \text{in } \hat{\Omega} \times (0, T), \tag{3}$$

where $\hat{\rho}_w$ is the density of water, and $\hat{\boldsymbol{u}} = \hat{\boldsymbol{u}}_w - \hat{\boldsymbol{u}}_s$.

The relative velocity $\hat{\boldsymbol{u}}$ of water $\hat{\boldsymbol{u}}_w$ with respect to that of the solid matrix $\hat{\boldsymbol{u}}_s$ is related to the pore pressure $\hat{p}$ by Darcy's law, i.e.

$$\hat{\phi}\hat{\boldsymbol{u}} = -\hat{J}\frac{\widetilde{\boldsymbol{K}}}{\mu_w}\left(\hat{\nabla}\hat{p} - \hat{\rho}_w \hat{\boldsymbol{F}}^T \boldsymbol{g}\right) \qquad \text{in } \hat{\Omega} \times (0, T), \tag{4}$$

with $\boldsymbol{g} = -g\boldsymbol{e}_z$. Here μ_w denotes the water viscosity and $\widetilde{\boldsymbol{K}} := \hat{\boldsymbol{F}}^{-1} \boldsymbol{K}(\hat{\phi}) \hat{\boldsymbol{F}}^{-T}$, where the permeability tensor $\boldsymbol{K}$ is assumed to be isotropic, thus

$$\boldsymbol{K}(\phi) = \mathcal{K}(\phi)\boldsymbol{I} \tag{5}$$

being $\mathcal{K}(\phi)$ given by the following relation, see [3],

$$\mathcal{K}(\phi) = \begin{cases} k_0\phi^3 \text{ if} & \phi \geq 0.1 \\ \dfrac{100\ k_0\phi^5}{(1-\phi)^2} \text{ if} & \phi < 0.1 \end{cases}. \tag{6}$$

Mechanical compaction of porous media is usually modeled by a relation between porosity and effective vertical stress known as Athy's law, [1]. However, in the case of our interest, porosity depends also on the concentration of precipitated mineral. According to [15], we model the coupled effect of dissolution/precipitation and compaction with the following equation,

$$\hat{\phi} = (\phi_0 + (1-\phi_0)(\hat{C}_0 - \hat{C}))\ e^{-\beta\hat{\sigma}}, \tag{7}$$

which is a generalization of Athy's law. Here, $\hat{\sigma}$ denotes the vertical effective stress defined as $\hat{\sigma} = \hat{s} - \hat{p}$, where $\hat{s}$ is the overburden and can be obtained integrating the differential equation

$$\frac{\partial \hat{s}}{\partial \xi} = -[(1-\hat{\phi})\hat{\rho}_s + \hat{\phi}\hat{\rho}_w]\ g\hat{J} \tag{8}$$

with the boundary condition $\hat{s}(x, \xi_{top}, t) = s_{\text{top}}(t)$, where s_{top} is a given function of time and accounts for the weight of the overlying layers. The density ρ_s of the solid matrix is obtained as the average of the density of the inert part of the rock ρ_r and that of the precipitated mineral $\hat{\rho}_p$, weighted with their volume fractions, that is

$$\hat{\rho}_s = \frac{(1-\hat{C}_0)\hat{\rho}_r + \hat{C}\hat{\rho}_p}{1-\hat{C}_0+\hat{C}}. \tag{9}$$

The equations (3), (4), (7), and (8) describe the coupling between water flow and compaction. We now introduce the chemical reactions that model the precipitation and dissolution of the transported mineral specie. Let us introduce the field $\hat{\gamma}$ that represents the dissolved mineral concentration in terms of moles per unit volume of water. The dissolved mineral is allowed to diffuse, to be transported by the fluid flow and to interact with the solid matrix, i.e. to precipitate, behaving as prescribed by the following equation:

$$\frac{\partial}{\partial t}(\hat{\gamma}\hat{\phi}\hat{J}) + \hat{\nabla}\cdot\left(\hat{\phi}\hat{\gamma}\hat{\boldsymbol{u}} - D\hat{\phi}\hat{\boldsymbol{F}}^{-T}\hat{\nabla}\hat{\gamma}\right) = r(\hat{C},\hat{\gamma})\hat{\phi}\hat{J} \qquad \text{in } \hat{\Omega}\times(0,T), \tag{10}$$

where $D > 0$ is the diffusion coefficient and $r(\hat{C},\hat{\gamma})$ is a source/well term that represents the dissolution/precipitation rate of the mineral. We point out that, since we are considering low velocities, we are here neglecting the effect of dispersion.

On the other hand, a source/sink term for equation (10) implies a sink/source term for the equation of the volume fraction of the precipitated mineral $\hat{C}$, as stated by the following equation:

$$\frac{\partial \hat{C}}{\partial t} = -V_m r(\hat{C},\hat{\gamma})\hat{\phi}, \tag{11}$$

where V_m is the molar volume of the mineral.

Following [2], we model the reaction rate r as a discontinuous function of γ and C. Let us introduce the following notation

$$x^+ := \max(0,x), \quad x^- := (-x)^+.$$

We model the source/sink term for the equations (10) and (11) as

$$r(C,\gamma) = \lambda \left(\text{sign}(C)^+ F(\gamma)^- - F(\gamma)^+\right), \tag{12}$$

where

$$F(\gamma) = \frac{\gamma}{\gamma_{eq}} - 1, \quad \gamma_{eq} > 0.$$

Here, γ_{eq} denotes an equilibrium concentration of the dissolved mineral. The rate constant λ is modeled according to Arrhenius law as

$$\lambda = \bar{\lambda} e^{-\frac{E}{RT}} > 0,$$

where E is an activation energy, R is the gas constant and the temperature T is assumed to be a given function of time.

We observe that, if the solute concentration exceeds the equilibrium value, $\gamma > \gamma_{eq}$, then $F(\gamma) > 0$ and $r = -\lambda\left(\frac{\gamma}{\gamma_{eq}} - 1\right) < 0$. In this case, precipitation occurs. On the other hand, if $\gamma < \gamma_{eq}$, then $F(\gamma) < 0$ and $r = \lambda\ \text{sign}(C)^+\left(1 - \frac{\gamma}{\gamma_{eq}}\right) \geq 0$. In this case, if $\text{sign}(C) > 0$ (i.e. if some precipitated is available in the rock), dissolution occurs. Finally, in case $\gamma = \gamma_{eq}$, $F(\gamma) = 0$ and the chemical equilibrium implies $r = 0$.

The solid mass conservation equation allows us to compute, knowing porosity and precipitate concentration, the velocity of the solid matrix and therefore the deformed configuration of the layer. Indeed, in this framework mass conservation of the solid phase in a porous medium implies

$$\frac{\partial}{\partial t}\left((1-\phi)\rho_s\right) + \frac{\partial}{\partial z}\left((1-\phi)\rho_s u_{sz}\right) = Q_s \qquad \text{in } \Omega(t) \times (0,T), \tag{13}$$

where Q_s is a source/sink term that models the growth or consumption of the solid grains, which can be shown to be

$$Q_s = \rho_p \frac{(1-\phi)}{1 - C_0 + C} \frac{DC}{Dt}. \tag{14}$$

To recover the deformed configuration of the layer, one can solve (13) for u_{sz} with a Dirichlet condition on the bottom boundary, and solve then $\frac{\partial z}{\partial t} = u_{sz}$ with a proper initial condition. We point out that, since we are considering the evolution of a single layer, such boundary conditions should be provided by the reconstruction of the history of the whole sedimentary basin.

The described system, complemented with suitable initial and boundary conditions, is a nonlinear system of strongly coupled equations. Indeed, it is clear that the changes in porosity can cause overpressures (i.e. pressures larger than hydrostatic) because permeability is a function of porosity, and moreover porosity plays a role in the storage term of fluid mass conservation. On the other hand, fluid pressure can counteract compaction reducing the effective vertical stress. Finally, chemical reactions are influenced by the fluid flow which transports the solute, and can increase or reduce the porosity if dissolution or precipitation occur. The approximation strategy implemented to tackle this coupling is illustrated in the next section.

3 The numerical approximation

For the solution of the coupled problem described in the previous section one could opt for a fully coupled approach using Newton iterations. However, even if a fully coupled approach is in general more robust, it is computationally very expensive and moreover the Jacobian matrix is likely to be ill-conditioned because of the different scales involved in the equations. For this reason we resort to an iterative splitting where the problems are solved in sequence, performing fixed point iterations until convergence is achieved.

3.1 Time discretization and iterative splitting

In principle all the aforementioned problems, i.e. fluid flow, compaction and solute dissolution/precipitation are coupled. If we assume that the effect of chemistry on porosity is moderate and relatively "slow" we can solve via fixed point iterations only the stronger coupling between pressure and compaction, and solve the advection, diffusion and reaction for the solute once per time step, reducing the computational cost. Therefore, for each time, we perform the following steps:

- integrate the chemical reactions and compute the solute using (10) and (11);
- enter the fixed point loop:
  - compute the sedimentary load and the effective stress with equation (8);
  - update of the porosity with equation (7);
  - solve Darcy's problem to obtain fluid pressure with equations (3) and (4);
  - check for convergence.

Since the reaction term in the ADR equation for γ is discontinuous, its approximation can benefit from a tailored integration scheme. Therefore it is very convenient, though not mandatory, to split the equation into an advection-diffusion part and a reaction part. This way, we can split the coupled problem of (10) and (11) into two sub-problems:

Advection-diffusion equation

$$\frac{\partial}{\partial t}(\hat{\gamma}\hat{\phi}\hat{J}) + \hat{\nabla}\cdot\left(\hat{\phi}\hat{\gamma}\hat{\boldsymbol{u}} - D\hat{\phi}\hat{\boldsymbol{F}}^{-T}\hat{\nabla}\hat{\gamma}\right) = 0 \tag{15}$$

Reaction system

$$\begin{cases} \dfrac{\partial\hat{\gamma}}{\partial t} = r(\hat{C},\hat{\gamma}) \\ \dfrac{\partial\hat{C}}{\partial t} = -V_m r(\hat{C},\hat{\gamma})\hat{\phi} \end{cases} \tag{16}$$

The two problems are solved in sequence according to a second order Strang splitting ([12, 14]). If we denote with $\hat{\gamma}^{n,n+1}$, $\hat{C}^{n,n+1}$ the concentrations at the discrete time t^n and t^{n+1} respectively, with $\hat{\gamma}^{*,**}$ two intermediate values of $\hat{\gamma}$ and with Δt the time step amplitude, the splitting consists in performing the following three steps

$$
\begin{aligned}
&I)\ \frac{2(\hat{\gamma}^*\hat{\phi}\hat{J} - \hat{\gamma}^n\hat{\phi}\hat{J})}{\Delta t} + \hat{\nabla}\cdot\left(\hat{\phi}\hat{\gamma}^*\hat{\boldsymbol{u}} - D\hat{\phi}\hat{\boldsymbol{F}}^{-T}\hat{\nabla}\hat{\gamma}^*\right) = 0\\
&II)\ \begin{cases} \dfrac{\hat{\gamma}^{**} - \hat{\gamma}^*}{\Delta t} = r(\hat{C}^n, \hat{\gamma}^*) \\ \dfrac{\hat{C}^{n+1} - \hat{C}^n}{\Delta t} = -V_m r(\hat{C}^n, \hat{\gamma}^*)\hat{\phi} \end{cases}\\
&III)\ \frac{2(\hat{\gamma}^{n+1}\hat{\phi}\hat{J} - \hat{\gamma}^{**}\hat{\phi}\hat{J})}{\Delta t} + \hat{\nabla}\cdot\left(\hat{\phi}\hat{\gamma}^{n+1}\hat{\boldsymbol{u}} - D\hat{\phi}\hat{\boldsymbol{F}}^{-T}\hat{\nabla}\hat{\gamma}^{n+1}\right) = 0.
\end{aligned}
$$

Note that we have chosen an implicit, thus more stable, discretization for the advection-diffusion part, while as concerns the reaction part an explicit scheme is more suitable for the implementation of the event detection method described in Section 3.3. We also point out that we are employing a higher order splitting to achieve better accuracy. Since for each time step we also need to solve some fixed point iterations for pressure and porosity, the use of an higher order splitting turns out to be more convenient than using a smaller the time step.

3.2 Finite element discretization

We have chosen a mixed finite element method for both the Darcy's problem and the advection-diffusion part of the equation for the solute concentration. This allows us to use the same finite element approximation for the relative velocity $\hat{\boldsymbol{u}}$ in equations (3) and (10). The finite element space chosen for the relative velocity $\hat{\boldsymbol{u}}$ is the lowest order Raviart Thomas $\mathbb{RT}_0(\hat{\Omega}, \mathcal{T}_h) \subset H(\mathrm{div}, \hat{\Omega})$, while the solute concentration γ and the water pressure p are in the space of the piece-wise constant functions $\mathbb{P}_0(\hat{\Omega}, \mathcal{T}_h) \subset L^2(\hat{\Omega})$. In both equations, since we are considering mixed formulations, the Dirichlet boundary conditions on pressure and concentration are naturally included in the weak formulation, while the Neumann boundary conditions on normal velocity and flux are imposed with a Nitsche's penalization technique (see [13]). Finally, the differential equation for the computation of the overburden s is solved with a SUPG stabilized finite element method, using $\mathbb{P}_1$ elements.

3.3 Numerical solution of the discontinuous ODEs for dissolution/precipitation

We now focus on the numerical approximation of the reaction part of the coupled problem (10), (11). Thanks to the splitting we can employ an *ad hoc* method for discontinuous ODEs. Indeed, once the problem has been discretized in space with the finite element method as described in the previous section, equations (16) become a system of ODEs for

each single degree of freedom. If we denote as $\hat{\boldsymbol{\gamma}}$, $\hat{\mathbf{C}}$ the vectors containing the degrees of freedom representing the solute and precipitate concentrations, being $\mathbf{r}$ the corresponding vector of the reaction rates defined as in (12), the two equations (10), (11) make up an ODE system with discontinuous right hand side, to whom Filippov theory can be applied. To this purpose, we define

$$\boldsymbol{y} = \begin{bmatrix} \hat{\boldsymbol{\gamma}} \\ \hat{\mathbf{C}} \end{bmatrix} \qquad \text{and} \qquad \boldsymbol{f} = \begin{bmatrix} \mathbf{r} \\ -V_m \mathbf{r} \hat{\phi} \end{bmatrix},$$

and we observe that

$$\frac{\partial y_i}{\partial t} = \begin{cases} f_i^1 & C = 0 \text{ and } \gamma_i < \gamma_{eq} \\ f_i^2 & \text{elsewhere} \end{cases}, \tag{17}$$

where

$$\boldsymbol{f}^1 = \begin{bmatrix} 0 \\ 0 \end{bmatrix} \qquad \text{and} \qquad \boldsymbol{f}^2 = \begin{bmatrix} \lambda \left(1 - \frac{\gamma}{\gamma_{eq}}\right) \\ -\lambda \phi V_m \left(1 - \frac{\gamma}{\gamma_{eq}}\right) \end{bmatrix}.$$

Numerical methods for the integration of DRH-systems can deal with the discontinuity with different approaches, such as step adaptation, or smoothing of the right hand side. The computational approach used in this work, proposed by [6], is designed to locate with accuracy the points where the transition occurs and check the transversality/sliding conditions of [6] through the following steps:

- integration of the ODE outside Σ, in particular, we use an explicit order 2 Runge Kutta method;
- location of the point $\mathbf{y} \in \Sigma$ reached by a trajectory, and the corresponding time t^* with an iterative method;
- check whether a crossing of the discontinuity has occurred;
- in case of sliding along the discontinuity, integration on Σ with the proper right hand side.

These steps are performed for each degree of freedom during the integration of (16) to achieve a good accuracy and, most of all, to avoid unphysical solutions such as the occurrence of negative concentrations.

4 Results

We simulate the compaction process of a $200m \times 120m$ sedimentary layer buried at the depth d. At the beginning of the simulation $d = d_0$, then a sedimentation velocity $\frac{\partial d}{\partial t} > 0$ brings the domain at a depth $d(t)$. We do not model the addition of extra layers due

to the progressive burial and the sedimentation acts only as a variation of the boundary conditions. For this reason, the boundary conditions for pressure and overburden are time-dependent. Temperature is a given field and is obtained with a geothermal gradient $\frac{\partial T}{\partial d}$ and a surface temperature T_0. The parameters used for the simulation are summarized in table 1.

	Value	Unit		Value	Unit		Value	Unit
β	10^{-8}	Pa^{-1}	ϕ_0	0.5	-	$\bar{\lambda}$	8.37 10^{-6}	$mol/(m^3\ s)$
d_0	2000	m	$\frac{\partial d}{\partial t}$	100	m/My	E	60.1	kJ/mol
T_0	20	°C	$\frac{\partial T}{\partial d}$	0.035	°C$/m$	γ_{eq}	0.167	mol/m^3
k_0	10^{-6}	$Darcy$	g	9.81	m/s^2	$\bar{\rho}$	2500	kg/m^3
μ_w	0.001	$Pa\ s$	D	1.58 10^{-8}	m^2/s	ρ_d	2500	kg/m^3
ρ_w	1000	kg/m^3	V_m	0.0226	m^3/mol	ρ_m	2660	kg/m^3

Table 1: Physical parameters for the simulation.

The numerical setup of this simulation is shown in figure 1. We have set for pressure hydrostatic Dirichlet boundary conditions at the top of the domain and at the bottom. The domain is considered as a part of a longer thin layer of rock, lying along the x-direction, hence no-flux boundary conditions are imposed on the lateral edges. A Dirichlet condition for the overburden is set at the top and we assume that the bottom of the domain moves downwards with a given, and in our case uniform, velocity. Finally, the dissolved mineral concentration is prescribed both at the top of the domain, where it is greater than that of equilibrium, and at the bottom, where it is equal to zero.

The rock is initially filled with water with no dissolved mineral ($\gamma_0 = 0$). The initial condition for pressure is the hydrostatic pressure and the initial conditions for stress and porosity are computed with some fixed point iterations of the stationary problem. The initial distribution of the precipitated mineral in the rock is sketched in figure 1. Finally, $\hat{\boldsymbol{u}}^0 = \mathbf{0}$.

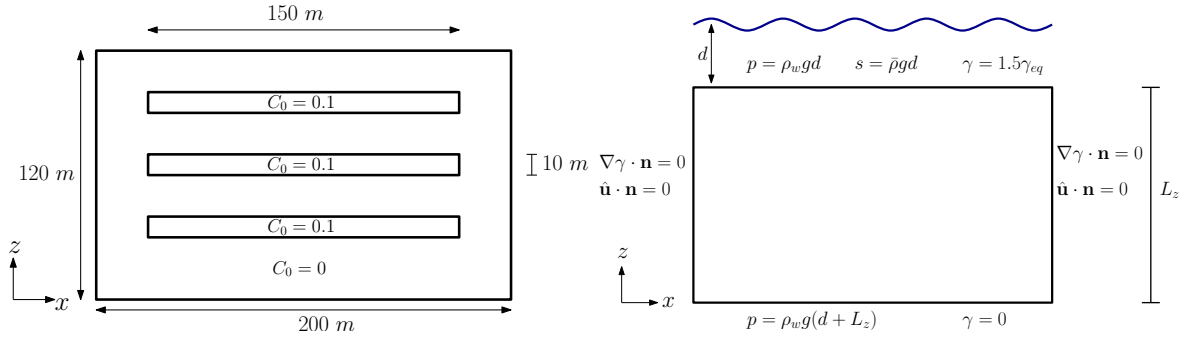

Figure 1: Numerical setup.

We solve the problem on a triangular mesh 50×30 with time step $\Delta t = 0.5\ 10^{11}\ s \approx 1.5\ ky$ to simulate a time span of $T = 25\ My$.

As expected, the mineral in water starts immediately to precipitate at the top of the domain, where its concentration is higher than that of equilibrium. At the same time, the precipitated mineral in rock dissolves in the lower region, where $\gamma < \gamma_{eq}$, behavior which lasts as long as there is mineral in rock that can dissolve, see Figure 2.

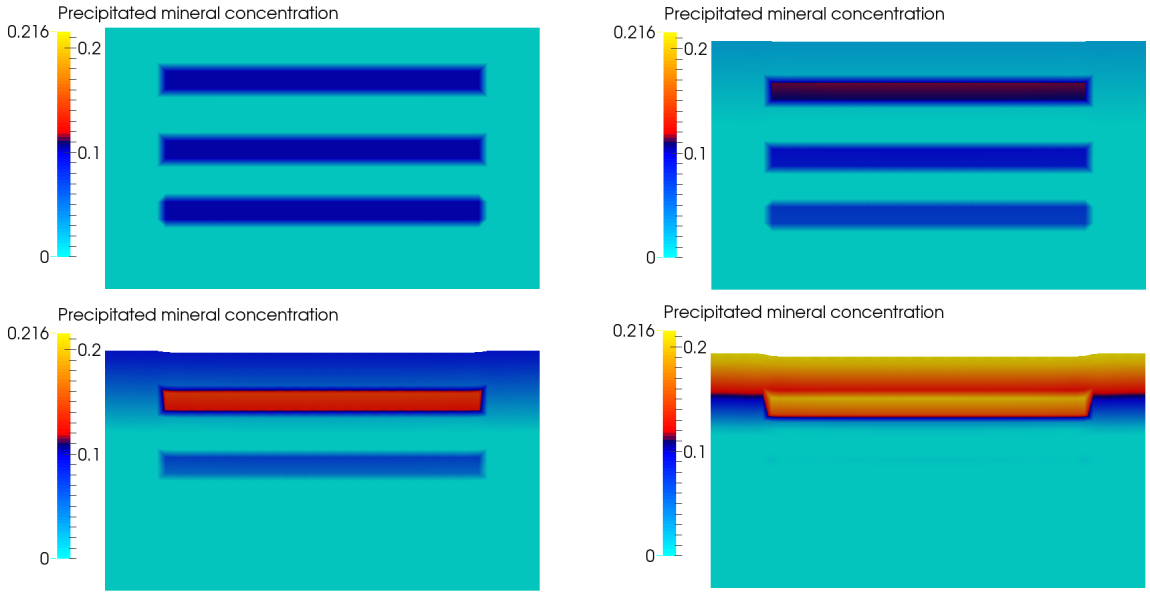

Figure 2: Plot of C at $t = 0$, $t = 8\ My$, $t = 16\ My$, and $t = 24\ My$ on the physical domain $\Omega(t)$.

In Figure 3, the porosity is shown, which decreases during the simulation due to the increase of overburden. An higher porosity is obtained, as expected, where the mineral originally present on the rock dissolves, since the dissolving mineral leaves some void spaces. On the other hand, porosity is lower at the top of the domain, where the mineral precipitates. Due to the non-uniform porosity, the domain compacts in a non-uniform way and we can clearly see at the end of the simulation that the region in which precipitated mineral has dissolved compacts more than its neighbor region.

5 Conclusion

We have proposed and tested a discretization method for the simulation of compaction in porous media with a particular focus on the numerical treatment of the discontinuous reaction terms that may arise in the modeling of geochemical processes. Even if we are considering a simplified model where only one mineral is allowed to precipitate, dissolve and be advected by the water flow, the results are qualitatively correct and the rigorous treatment of the discontinuity avoids the occurrence of negative concentrations and oscillations. The whole approximation strategy has been developed with the aim of finding

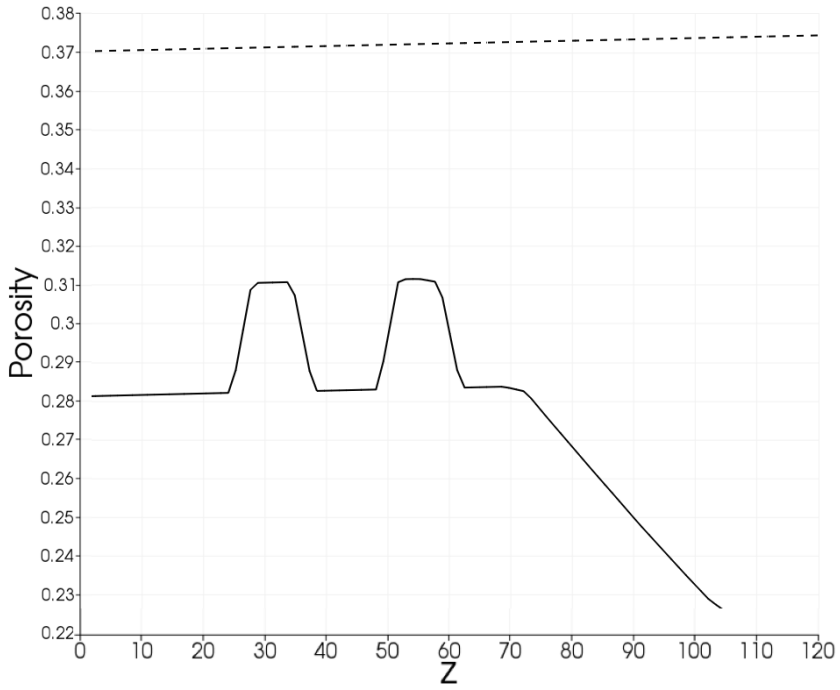

Figure 3: Plot of porosity versus z at $t = 0$, $t = 8\ My$, $t = 16\ My$, and $t = 24\ My$, taken on the vertical line that halves the domain. The dashed and the solid lines represent the initial and the final porosity respectively.

a trade-off between accuracy and computational efficiency. However, there is still room for improvement: in particular a more precise assessment of the error introduced by the splittings will be the subject of future work.

REFERENCES

[1] L. F. Athy. Density, porosity, and compaction of sedimentary rocks. *AAPG Bulletin*, 14(1):1–24, 1930.

[2] N. Bouillard, R. Eymard, R. Herbin, and P. Montarnal. Diffusion with dissolution and precipitation in a porous medium: mathematical analysis and numerical approximation of a simplified model. *ESAIM: Mathematical Modelling and Numerical Analysis*, 41:975–1000, 2007.

[3] Z. Chen, R. E. Ewing, H. Lu, S. L. Lyons, S. Maliassov, M. B. Ray, and T. Sun. Integrated two-dimensional modeling of fluid flow and compaction in a sedimentary basin. *Computational Geosciences*, 6:545–564, 2002.

[4] M.F. Danca. On the uniqueness of solutions to a class of discontinuous dynamical systems. *Nonlinear analysis: real world applications.* in press, doi:10.1016/j.norwa.2009.02.024.

[5] L. Dieci and L. Lopez. A survey of numerical methods for ivps of odes with discontinuous right-hand side. *Journal of Computational and Applied Mathematics*, 236(16):3967–3991, October 2012.

[6] Luca Dieci and Luciano Lopez. Numerical solution of discontinuous differential systems: Approaching the discontinuity surface from one side. *Applied Numerical Mathematics*, 67:98–110, 2013.

[7] A. C. Fowler and X. S. Yang. Dissolution/precipitation mechanisms for diagenesis in sedimentary basins. *Journal of Geophysical Research: Solid Earth (1978–2012)*, 108(B10), 2003.

[8] C. W. Gear and O. Østerby. Solving ordinary differential equations with discontinuities. *ACM transaction on mathematical software*, 10(1):23–24, 1984.

[9] B. Giovanardi, A. Scotti, L. Formaggia, and P. Ruffo. *A general framework for the simulation of geochemical compaction.* Mox Report, 2015.

[10] K. Kumar, I.S. Pop, and F.A. Radu. Convergence analysis of mixed numerical schemes for reactive flow in a porous medium. *SIAM Journal on Numerical Analysis*, 51(4):2283–2308, 2013.

[11] R. H. Lander and O. Walderhaug. Predicting porosity through simulating sandstone compaction and quartz cementation. *AAPG bulletin*, 83(3):433–449, 1999.

[12] D. Lanser and J. G. Verwer. Analysis of operator splitting for advection–diffusion-reaction problems from air pollution modelling. *Journal of Computational and Applied Mathematics*, 111(12):201 – 216, 1999.

[13] J. Nitsche. Über ein Variationsprinzip zur Lösung von Dirichlet-Problemen bei Verwendung von Teilräumen, die keinen Randbedingungen unterworfen sind. *Abhandlungen aus dem Mathematischen Seminar der Universität Hamburg*, 36:9–15, 1971.

[14] D. L. Ropp and J. N. Shadid. Stability of operator splitting methods for systems with indefinite operators: Advection-diffusion-reaction systems. *Journal of Computational Physics*, 228(9):3508 – 3516, 2009.

[15] M. Wangen. Vertical migration of hydrocarbons modelled with fractional flow theory. *Geophysical Journal International*, 115:109–131, 1993.

[16] M. Wangen. Two-phase oil migration in compacting sedimentary basins modelled by the finite element method. *International Journal for Numerical and Analytical Methods in Geomechanics*, 21:91–120, 1997.